

FLUID - RIGID BODY INTERACTION BY PETSC-FEM DRIVEN BY PYTHON

Germán Filippini^a, Lisandro Dalcin^a, Norberto Nigro^a and Mario Storti^a

^aCentro Internacional de Métodos Computacionales en Ingeniería (CIMEC) INTEC(CONICET-UNL),
Güemes 3450, (S3000GLN), Santa Fe, Argentina

<http://www.cimec.org.ar>

e-mail: gfilippini@santafe-conicet.gov.ar

Keywords: fluid-rigid body interaction, vortex-induced vibration, Lock-In phenomenon.

Abstract. Fluid structure interaction (FSI) involving rigid bodies contains three main problems to be solved, the computational fluid dynamics (CFD), the computational mesh dynamics (CMD) and the multi-body dynamics (MBD). Python is used as a glue language capable of connecting this three main problems in a high-level, interactive and productive environment. This interaction is implemented in PETSc-FEM code (<http://www.cimec.org.ar/petscfem>) which is a parallel multi-physics finite element based on PETSc. PETSc is a suite of data structures and routines for the scalable solution of scientific applications modeled by partial differential equations. It employs the MPI standard for all message-passing communication. PETSc for Python (petsc4py) are Python bindings for PETSc used in this work.

A stabilized ALE (Arbitrary Lagrangian-Eulerian) formulation is used to solve the incompressible laminar Navier Stokes equations in a moving grid. The mesh dynamics may be solved in general by a global optimization strategy, however, in some special cases, a simple ad-hoc procedure may be adopted. For each subproblems a second order accurate in time scheme is adopted. Results for vortex-induced vibrations (VIV), galloping and flutter of some numerical examples at low Reynolds number are presented.

1. INTRODUCTION

Multiphysics relates to the interaction between systems with different physical behaviors, the interaction between fluid and structure is an example of this. Both systems interact in the contours of their domains they share. In our particular case study the contour of the structure is not deformable, since we are interested in studying multibody systems with their own dynamics given by their inertia and structural characteristics, immersed in a fluid flow.

Basically there are two ways of modeling multiphysics problems, Monolithic (Simultaneous Treatment) and Partitioned Treatment. In the first case, the whole problem is treated as a monolithic entity, and all components advanced simultaneously in time. In the Partitioned Treatment, the field models are computationally treated as isolated entities that are separately stepped in time. Interaction effects are viewed as forcing terms that are communicated among individual components using prediction, substitution and synchronization techniques. We favour the partitioned treatment since it allows *customization, independent modeling, software reuse and modularity*. However the partitioned approach requires careful formulation and implementation to avoid degradation in stability and accuracy (Storti et al., 2006).

Fluid flow is naturally modeled by FEM, depending on their physical characteristics (flow, turbulence, moving boundaries, etc.). Multibody systems are modeled through a series of ODE's.

To solve the flow of fluid we use the program PETSc-FEM, which is a parallel multiphysics finite element based on PETSc. PETSc is a suite of data structures and routines for the scalable solution of scientific applications modeled by partial differential equations. It employs the MPI standard for all message-passing communication.

Of the many methods in the bibliography for modeling multibody dynamics, we used a method called Bond Graphs (BG). BG's represent elementary energy-related phenomena (generation, storage, dissipation, power exchange) using a small set of ideal elements that can be coupled together through external ports representing power flow (Karnopp et al., 2000).

Besides the computational fluid dynamics (CFD) and the multi-body dynamics (MBD), in this type of interaction it is necessary to resolve the computational mesh dynamics (CMD).

Python is used as a glue language capable of connecting these three main problems in a high-level, interactive and productive environment.

2. GENERAL SPECIFICATIONS

2.1 Fluid Dynamics

Because the fluid and the solid domains move arbitrarily it may be necessary to define a moving reference frame in which the conservation laws are formulated. This strategy is established through the Arbitrary Lagrangian Eulerian (ALE) formulation.

Viscous flow is well represented by Navier-Stokes equations. The incompressible version of this model includes the mass and momentum balances that can be written in the following form. Let $\Omega \in R^{Nsp}$ and $(0, t_+)$ be the spatial and temporal fluid domains respectively, where Nsp is the number of space dimensions, and let Γ be the boundary of Ω , both of them to be defined later. The operator $\nabla_{\hat{x}}(\cdot)$ denotes the derivative with respect to the current referential coordinates \hat{x} and $\dot{\mathbf{u}}$ corresponds to the change of the material particle velocity noted by an observer traveling with the referential coordinate. Therefore,

$$\nabla_{\hat{x}} \cdot \mathbf{u} = 0 \quad \text{in } \Omega \times (0, t_x) \quad (1)$$

$$\rho (\dot{\mathbf{u}} + (\mathbf{u} - \hat{\mathbf{v}}) \cdot (\nabla_{\hat{x}} \mathbf{u}) - \mathbf{f}) - \nabla_{\hat{x}} \cdot \boldsymbol{\sigma} = 0 \quad \text{in } \Omega \times (0, t_x) \quad (2)$$

with ρ and \mathbf{u} the density and velocity of the fluid, \mathbf{f} the volume force vector, the velocity difference $(\mathbf{u} - \hat{\mathbf{v}})$ is commonly called the *convective velocity* and $\boldsymbol{\sigma}$ the stress tensor, given by

$$\boldsymbol{\sigma} = -p \mathbf{I} + 2\mu^* \boldsymbol{\epsilon}(\mathbf{u}) \quad (3)$$

$$\boldsymbol{\epsilon}(\mathbf{u}) = \frac{1}{2}(\nabla_{\hat{x}} \mathbf{u} + (\nabla_{\hat{x}} \mathbf{u})^t) \quad (4)$$

where p is the pressure and μ^* is the effective dynamic viscosity defined as sum of the dynamic (molecular) viscosity and the algebraic eddy viscosity coming from the turbulence model. \mathbf{I} represents the identity tensor and $\boldsymbol{\epsilon}$ the strain rate tensor.

2.2 Multibody Dynamics

Each rigid body has a set of three equations associated with the 3 dof's for 2D, two for each components of the linear momentum conservation and the reminder account for the conservation of angular momentum. Linear and angular inertia, damping and stiffness characterize the rigid body motion assuming for simplicity that the behavior is linear and uncoupled.

$$m_i^k \ddot{d}_i^k + c_i^k \dot{d}_i^k + k_i^k d_i^k = F_i^k \quad (5)$$

$$I_\theta^k \ddot{\theta}^k + c_\theta^k \dot{\theta}^k + k_\theta^k \theta^k = M^k \quad (6)$$

where i means the coordinate direction x, y and k is an index along the whole set of rigid bodies. The displacements d_i^k are the components of the k rigid body translation $d^k = \{d_x^k, d_y^k\}$ whereas θ^k describes the k rigid body rotation with respect to its gravity center G . The scalar quantities $m_i, c_i, k_i, I_\theta, c_\theta$ and k_θ denote the mass, the damping and the stiffness constant for the translational and rotational degrees of freedom, respectively. The scalars F_i represent the components of the force vector, while M is the moment.

A typical description of the rigid body dynamics problem may be viewed in figure 1. The initial position of a typical rigid body is defined through the gravity center G_0 , locate relative to an inertial reference frame (X, Y) by position vector \mathbf{r}_0 , and the body fixed reference frame (X_0, Y_0) . A typical point at its surface is named P_0 . By the fluid forces and moments the rigid body moves to the current position defined by G , with the new position vector $\mathbf{r} = \mathbf{r}_0 + \delta \mathbf{r}$ and its new orientation given by (X', Y') rotated from the original orientation an angle θ . The point P_0 moves to its current location P with the new normal \mathbf{n} .

gravity center G. A detail of the two meshes and the interface is shown in figure 2

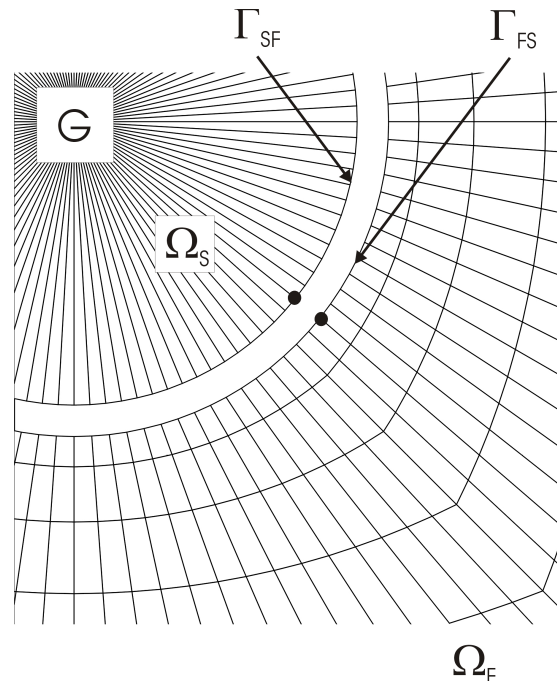


Figure 2: Meshes and discrete interfaces

3. LINKING BGS MODELS WITH PETSC-FEM THROUGH PYTHON

Bond Graphs have a concept of causality defining the order in which the mathematical equations of the mechanical model should be computationally solved.

Some end-user applications for BG modeling provide facilities for generating C or C++ codes implementing the required computations for simulating the BG models. Such codes can be easily accessed within a Python programming environment by employing appropriate tools like SWIG. SWIG is a software development tool that connects programs written in C and C++ with a variety of high-level programming languages. Then, as PETSc-FEM and BG models are driven by Python, it is possible to link them and solve this fluid-rigid body interaction.

4. STRONGLY COUPLED PARTITIONED STAGED ALGORITHM

For each subproblems a second order accurate in time scheme is adopted but different methods of coupling were implemented in this Python interface. The first and simplest is called Weak Coupling without Predictor. Then we implemented a predictor for the solid (*Weak Coupling with Predictor*) and the possibility of new loops within the loop of time step (*Stage Strong Coupling with Predictor*).

4.1 Weak Coupling without Predictor

- 1- Initialization: Solve Fluid
- 2- Time Step Loop:
 - (a) Compute Fluid Forces
 - (b) Solve Solid

- (c) *Compute Solid Displacements*
- (d) *Solve Mesh*
- (e) *Solve Fluid*

Staggered procedures are very effective for coupled first-order parabolic systems. For more general problems, particularly those modeled by oscillatory second order ODE's, the stability restriction can become serious. Weak coupling degrades the time-stepping stability; the new rigid body state is determined for the forces exerted by the fluid in the previous step.

4.2 Weak/Strong Stage Coupling with Predictor

In this coupling method a predictor is used. The general form of the predictor for the rigid body state was taken from reference (Piperno and Farhat, 2001) and can be written as

$$d^{(n+1)p} = d^{(n)} + \alpha_0 \Delta t \dot{d}^n + \alpha_1 \Delta t (\dot{d}^n - \dot{d}^{n-1}) \quad (7)$$

It is at least first order accurate when no predictor is employed and it may be improved to second order using the above predictor with some values for α_0 and α_1 . To understand the influences of these parameters a simple two *dofs* second order in time coupled ordinary differential equations model has been analyzed.

The algorithm is as follows:

- 1- *Initialization*
- 2- *Time Step Loop:*
 - (a) *Solve Solid Predictor*
 - (b) *Compute Solid Displacements*
 - (c) *Solve Mesh*
 - (d) *Stage Loop*
 - (i) *Solve Fluid*
 - (ii) *Compute Fluid Forces*
 - (iii) *Solve Solid*
 - (iv) *Compute Solid Displacements*
 - (v) *Solve Mesh*

Once satisfactory stability is achieved, the next concern is accuracy. This is usually degraded with respect to that attainable by the monolithic scheme. In principle this can be recovered by iterating the state between the fields. Iteration is done by cycling substitutions at the same time step.

5. NUMERICAL EXAMPLES

5.1 Vortex Induced Vibration

This example has been studied in a previous paper (Filippini et al., 2006) but now with the aim to validate this new interface PETSc-FEM driven by Python. The figure 3 shows the system under study, which consists of a cylinder immersed in a flow of fluid with a degree of freedom in the transverse direction to the flow.

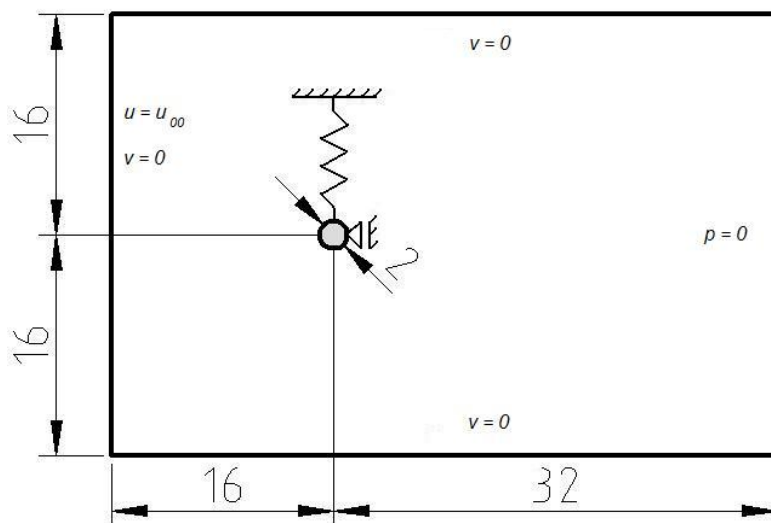


Figure 3: VIV Example

The domain is discretized in a mesh of triangles with 13048 elements and 7204 nodes. The mesh is refined near the skin of the body and in the wake as shown in figure 4. It is assumed that the cylinder has a mass $m=481.7877\text{kg}$, the spring is linear with the stiffness $k=1.4823 \times 10^{-4}\text{N/m}$ and a damping factor $c=6.4974 \times 10^{-4}\text{Ns/m}$. Then the mechanical system has a natural frequency $f_n=5.5467 \times 10^{-4}\text{s}^{-1}$. The fluid properties are set to $\mu=2 \times 10^{-5}\text{Ns/m}$ and $\rho=1\text{kg/m}^3$.

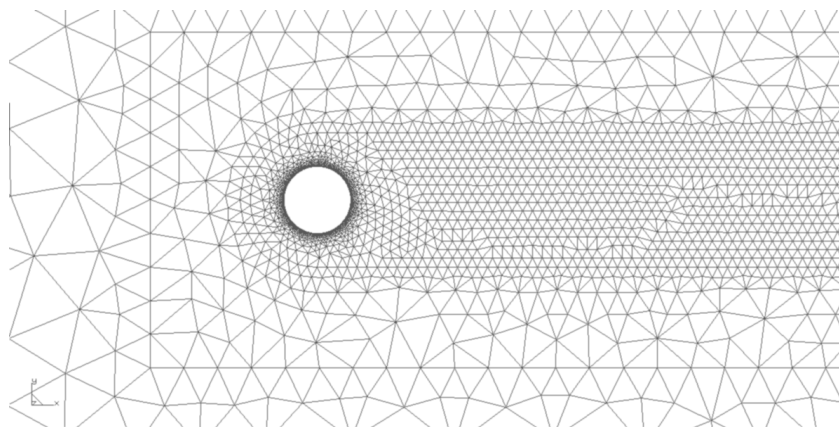


Figure 4: Mesh

The figure 5 shows the BG's model of the mechanical system. The symbol I in BG's represent the mass of the cylinder, the symbol C is a spring, R is a damper and MSe is a modulated source representing the force applied by the fluid on the mechanical system.

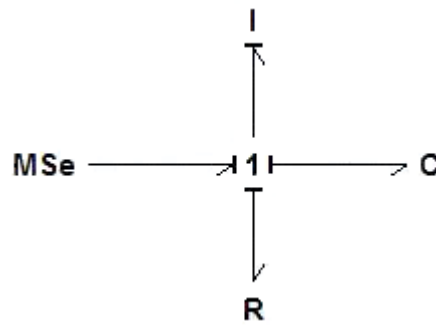


Figure 5: BGs Model

Simulations were performed for different Reynolds numbers in an interval between 90 and 140; the time step used was $dt=200s$. The characteristic behavior of this system is the *lock-in* phenomenon: there is an interval of free stream velocities for which the vortex shedding f_v agree with the natural frequency f_n of the cylinder-spring system. If U_∞ lies within this interval then the cylinder performs stable oscillations, with amplitudes as large as the cylinder diameter. Otherwise the oscillations are negligible. The existence of this lock-in region is an evidence for the two-way coupling between the fluid and the mechanical system. The fluid flow excites the oscillations of the cylinder, whereas the motion of the cylinder causes the *lock-in* effect altering the vortex shedding frequency f_v to be equal to the natural frequency f_n . This effect may be observed in figures 6 and 7. Figures 8, 10, 12 and 14 shows vertical fluid force for different Reynolds numbers. Figures 9, 11, 13 and 15 shows how the cylinder oscillation develops in time for different Reynolds numbers. Figure 16 shows the magnitude of the velocity at Reynolds 105 for a sequence of states where the *lock-in* is observed.

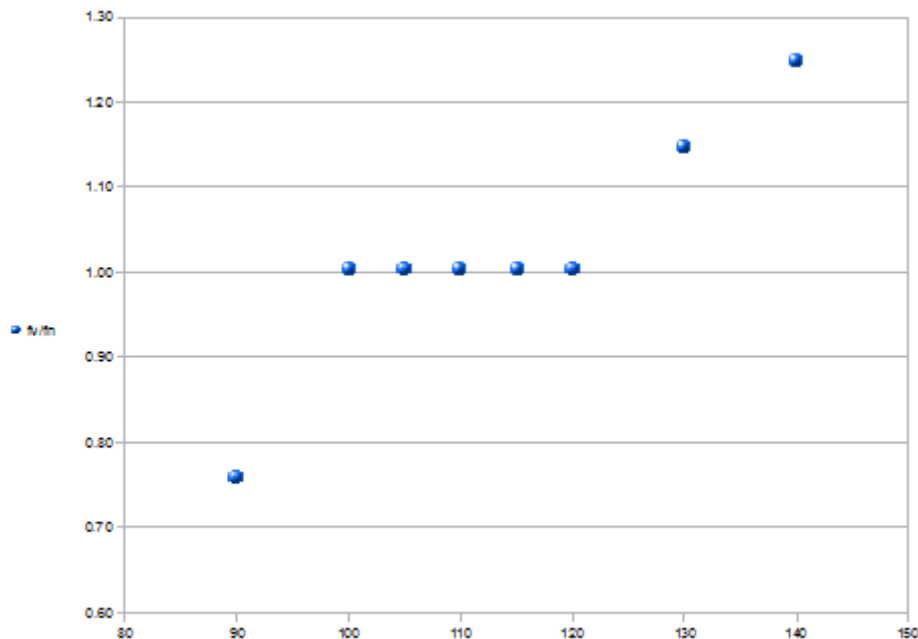


Figure 6: Frequency ratio vs Reynolds

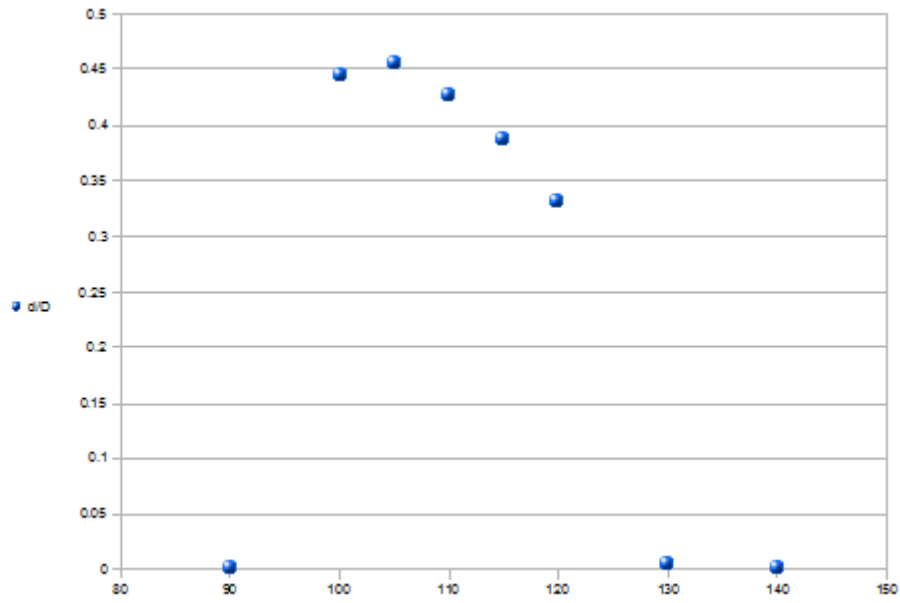


Figure 7: Amplitud ratio vs Reynolds

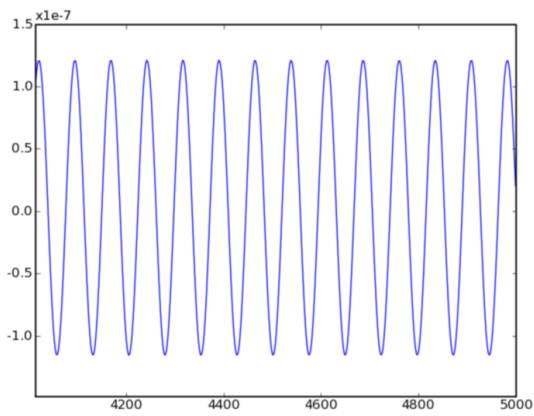


Figure 8: Vertical Force [N] - Re 90

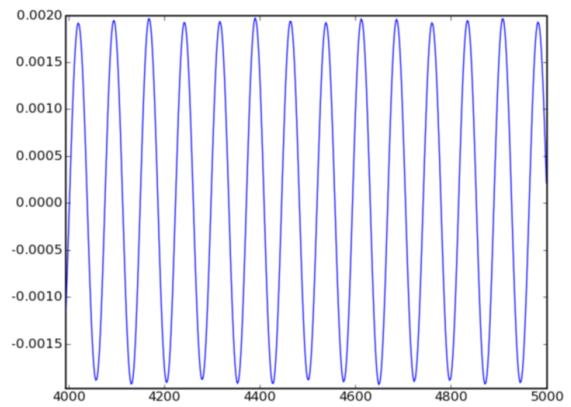


Figure 9: Vertical Displacement [m] – Re 90

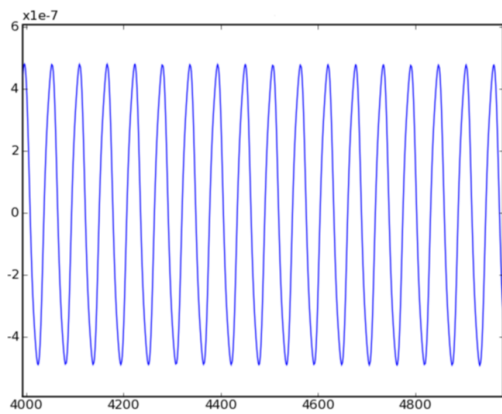


Figure 10: Vertical Force [N] - Re 105

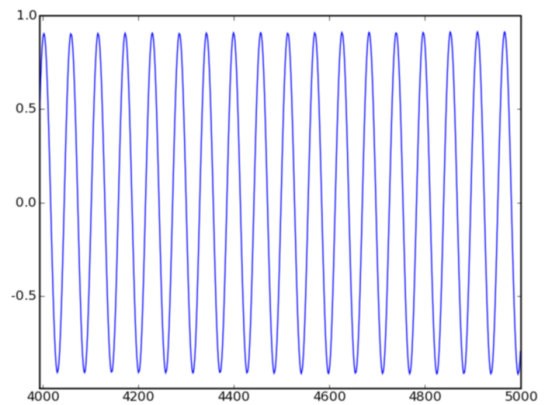


Figure 11: Vertical Displacement [m] – Re 105

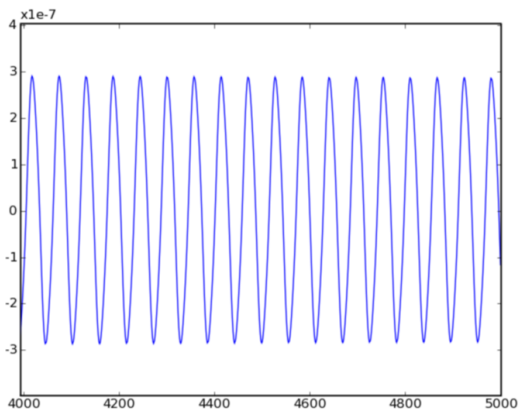


Figure 12: Vertical Force [N] - Re 120

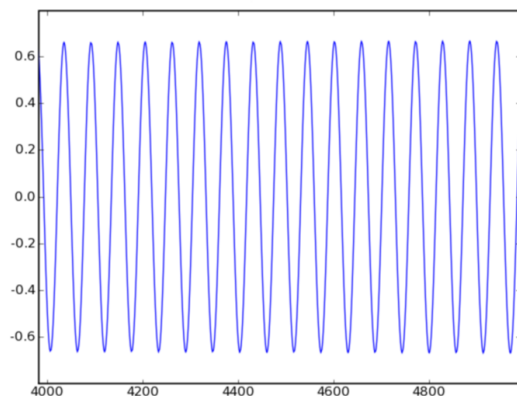


Figure 13: Vertical Displacement [m] – Re 120

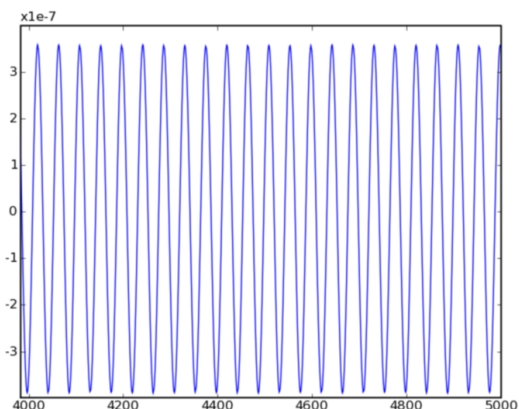


Figure 14: Vertical Force [N] – Re 140

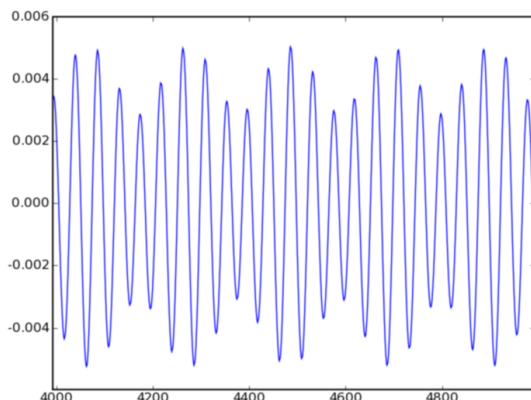
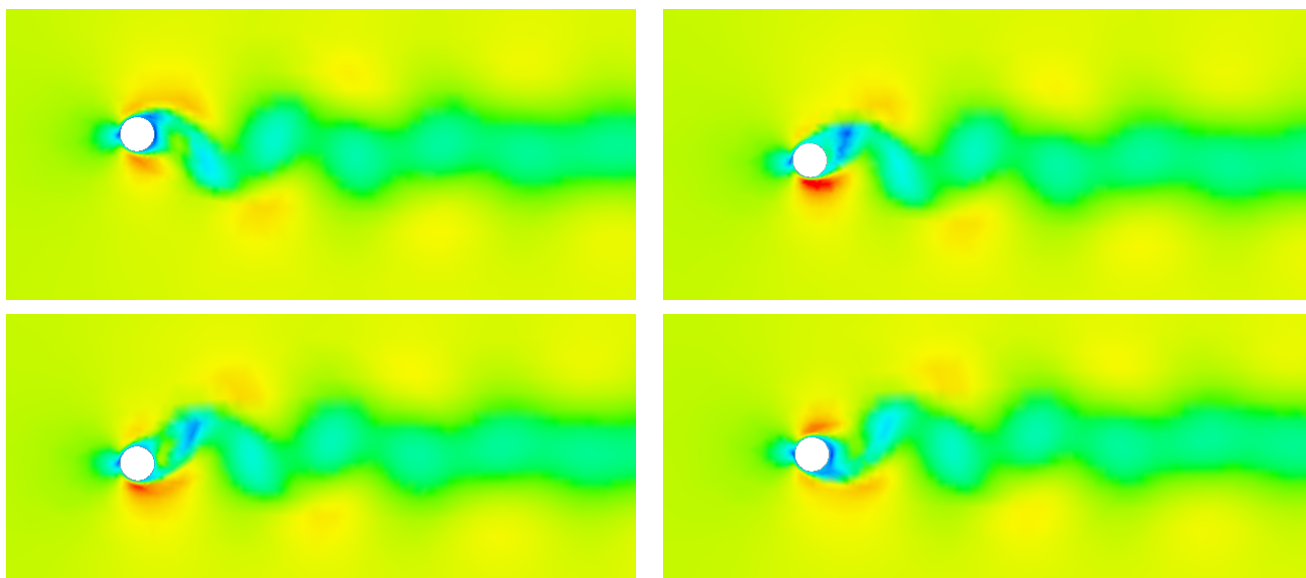


Figure 15: Vertical Displacement [m] – Re 140



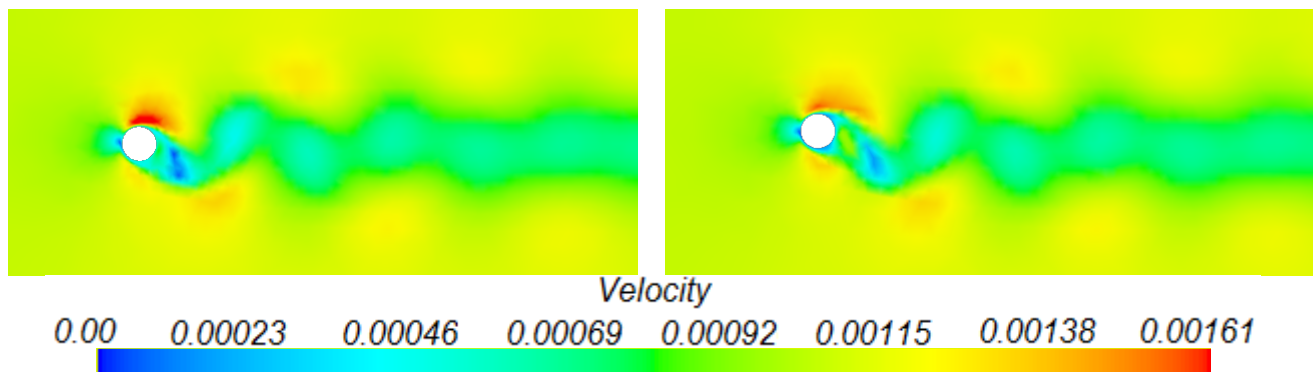


Figure 16: Magnitude of Velocity – Re 105

5.2 Galloping

Many flow induced vibrations happen at frequencies which are much smaller than the vortex shedding frequencies. In the case of mechanical systems with only one degree of freedom, this phenomenon is commonly denoted as *galloping* (Dettmet et al., 2006). The associated flow velocities are usually large. The mechanical explanation of *galloping* is presented, for instance, in Blevins (1977). Figure 17 shows the example study of *galloping*, which has a rotational degree of freedom.

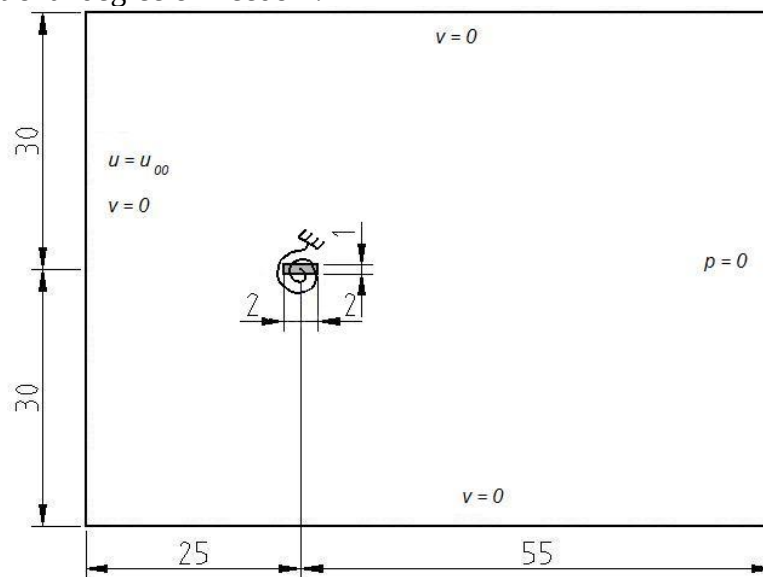


Figure 17: Galloping Example

A triangular mesh of 3600 elements and 1904 nodes is used. The mesh is refined near the skin of the body and in the wake as shown in figure 18. It is assumed that the body has an inertia $I_\theta=400kgm^2$, a linear torsion spring with a stiffness constant $k_\theta=61.685Nm$ and a damping factor $c_\theta=78.54Ns$. Then the mechanical system has a natural frequency $fn=0.0625$. They were chosen according to Dettmet et al. (2006). The BG's model of the mechanical system is equal to the previous example (figure 6) but for the case of rotation.

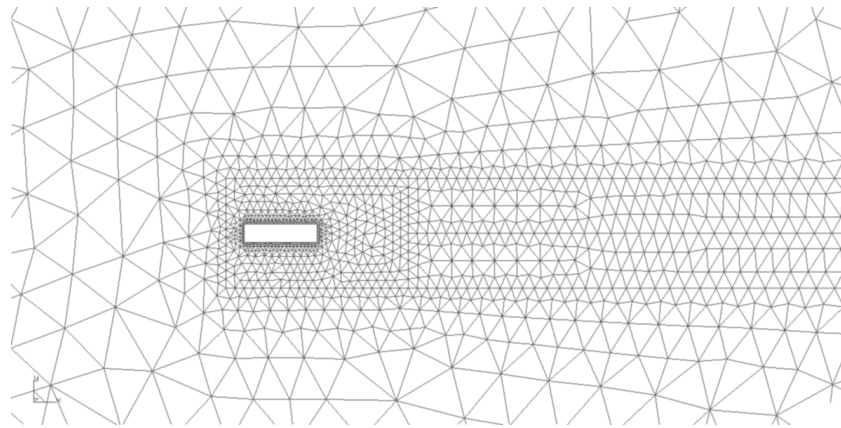


Figure 18: Mesh

The fluid properties are set to $\mu=0.01\text{Ns/m}$ and $\rho=1\text{kg/m}^3$ and the inflow velocity is $u_\infty=2.5\text{m/s}$, leading to a Reynolds numbers of 250. Figure 19 shows the angular momentum exerted by the fluid on the body. Figure 20 shows the angle of rotation. The vortex shedding frequency is $f_v=0.25(4f_n)$, while the frequency of oscillation $f_o=0.0588(0.94f_n)$. This range of frequency ratios ($f_v < f_n$ and $f_o \approx f_n$) is typical of a state of *galloping*. Figure 21 shows the magnitude of the velocity at Reynolds 250 for a sequence of states where the *galloping* is observed.

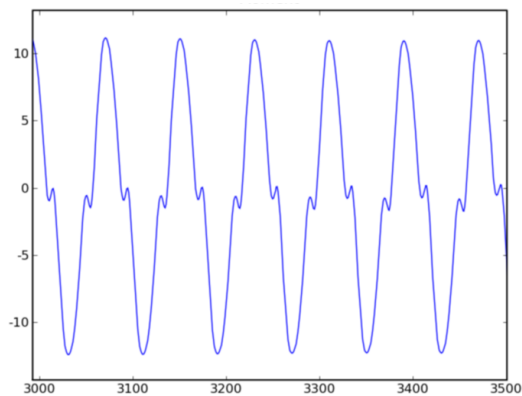


Figure 19: Angular Momentum [Nm]

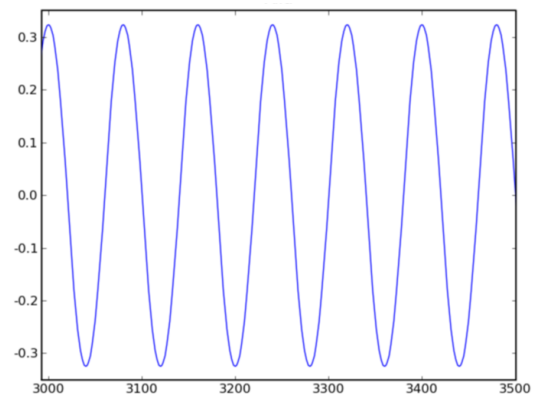
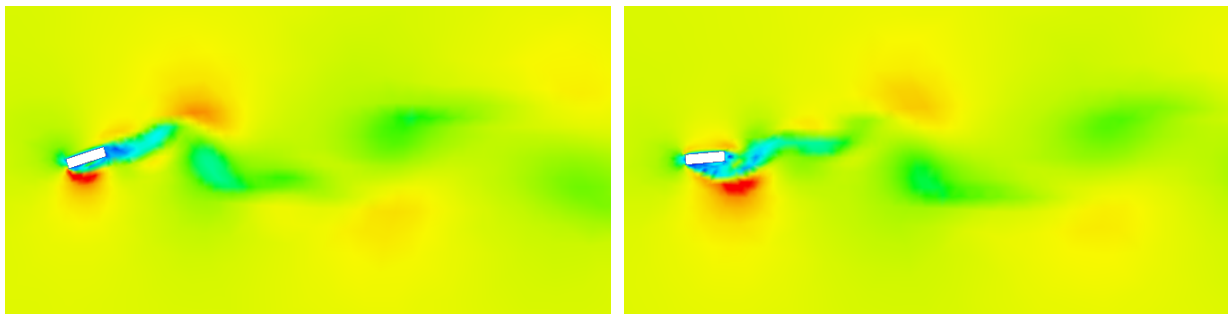


Figure 20: Angle of rotation [rad]



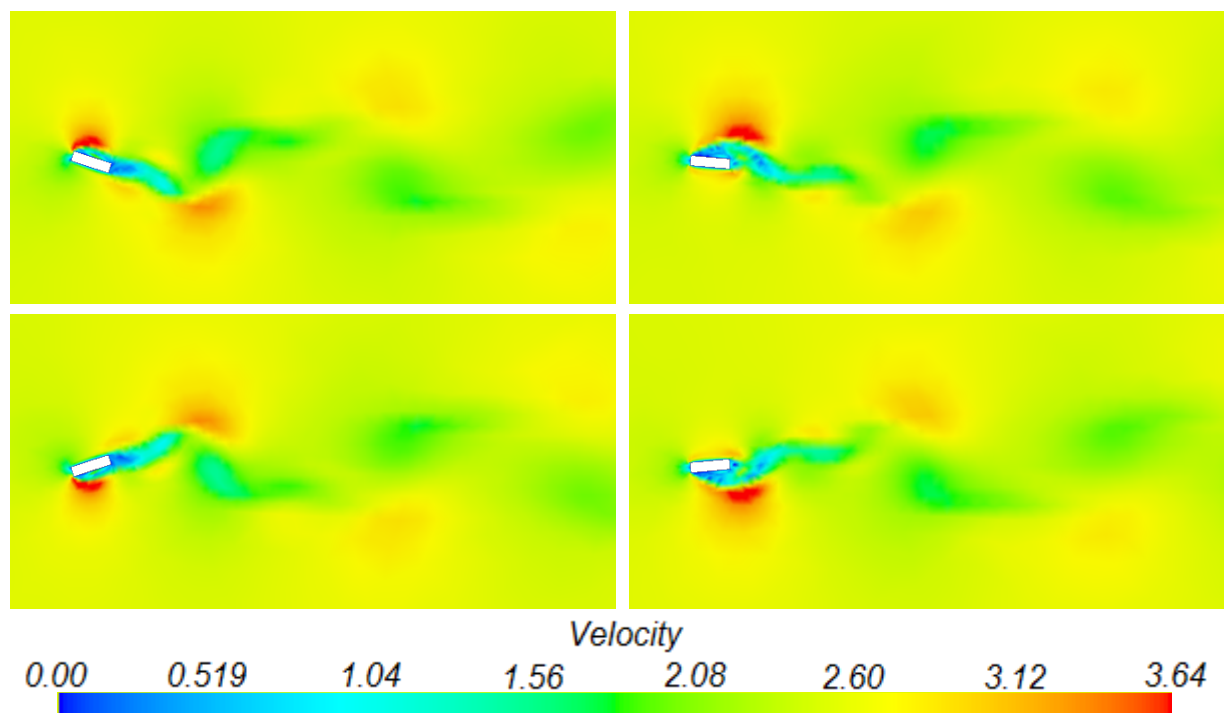


Figure 21: Magnitude of Velocity

5.3 Flutter

This is an example of a rigid H-profile supported with a rotational and a vertical translational lineal elastic spring. It's exposed to uniform fluid flow in the horizontal direction. This model problem, shown in figure 22, may be used to evaluate the aerodynamic stability of a suspension bridge. Coupled galloping of two or more degrees of freedom is commonly known as *flutter* (Dettmet et al., 2006).

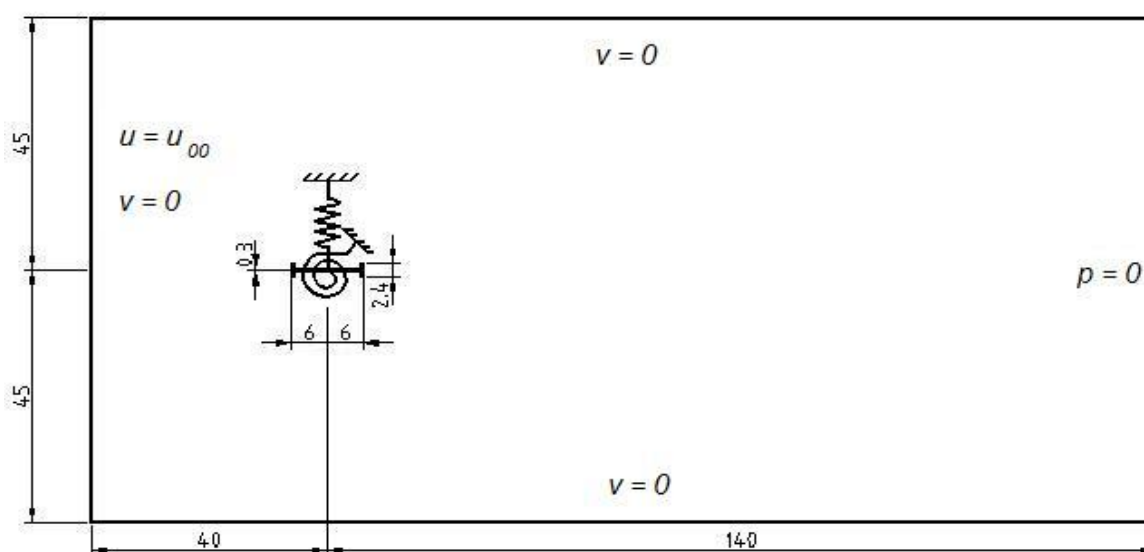


Figure 22: Flutter Example

Figure 23 shows the mesh used for this example. It has 3720 triangular elements and

1983 nodes. The body has a mass $m=3000\text{kg}$, the spring is linear with a stiffness constant $k=2000\text{N/m}$ and a damping factor $c=100\text{Ns/m}$. The body has a inertia $I_\theta=25300\text{kgm}^2$, the torsion spring is linear with a stiffness constant $k_\theta=40000\text{Nm}$ and a damping factor $c_\theta=2200\text{Ns}$. The mechanical system has a natural frequency $f_{yn}=0.130\text{s}^{-1}$ and $f_{\theta n}=0.2\text{s}^{-1}$.

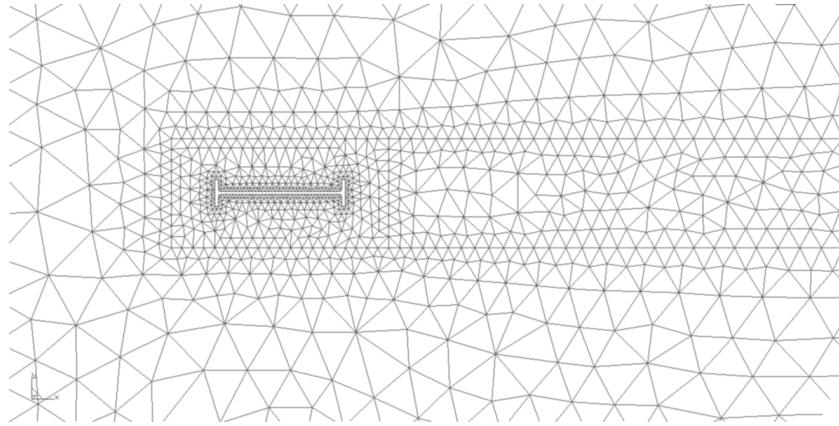


Figure 23: Mesh

The fluid properties are set to $\mu=0.1\text{Ns/m}$ and $\rho=1.25\text{kg/m}^3$ and the inflow velocity is $u_\infty=10\text{m/s}$. Figure 24 shows the vertical fluid force and figure 25 shows the vertical position of the body. Figure 26 shows the angular momentum exerted by the fluid on the body and figure 27 shows the angle of rotation. After a while the oscillations take a stable pattern. The amplitude of the rotation is 0.271 and the maxima of vertical displacements w_y are bounded between $0.39 < \max(w_y) < 0.42$. For this case the rotation is the dominant motion. Figure 28 shows the magnitude of the velocity for a sequence of states where *flutter* is observed.

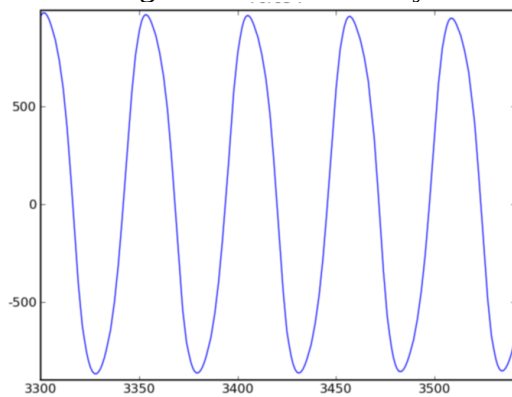


Figure 24: Vertical Force [N]

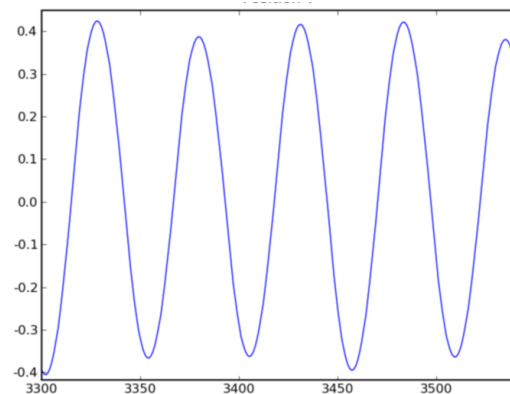


Figure 25: Vertical Displacement [m]

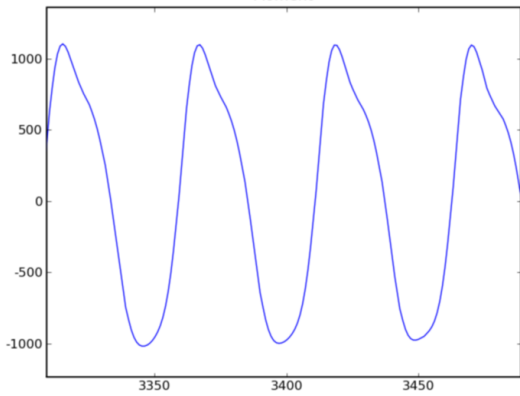


Figure 26: Angular Momentum [Nm]

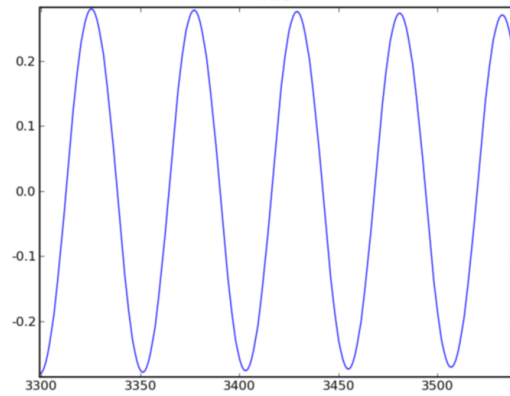


Figure 27: Angle of rotation [rad]

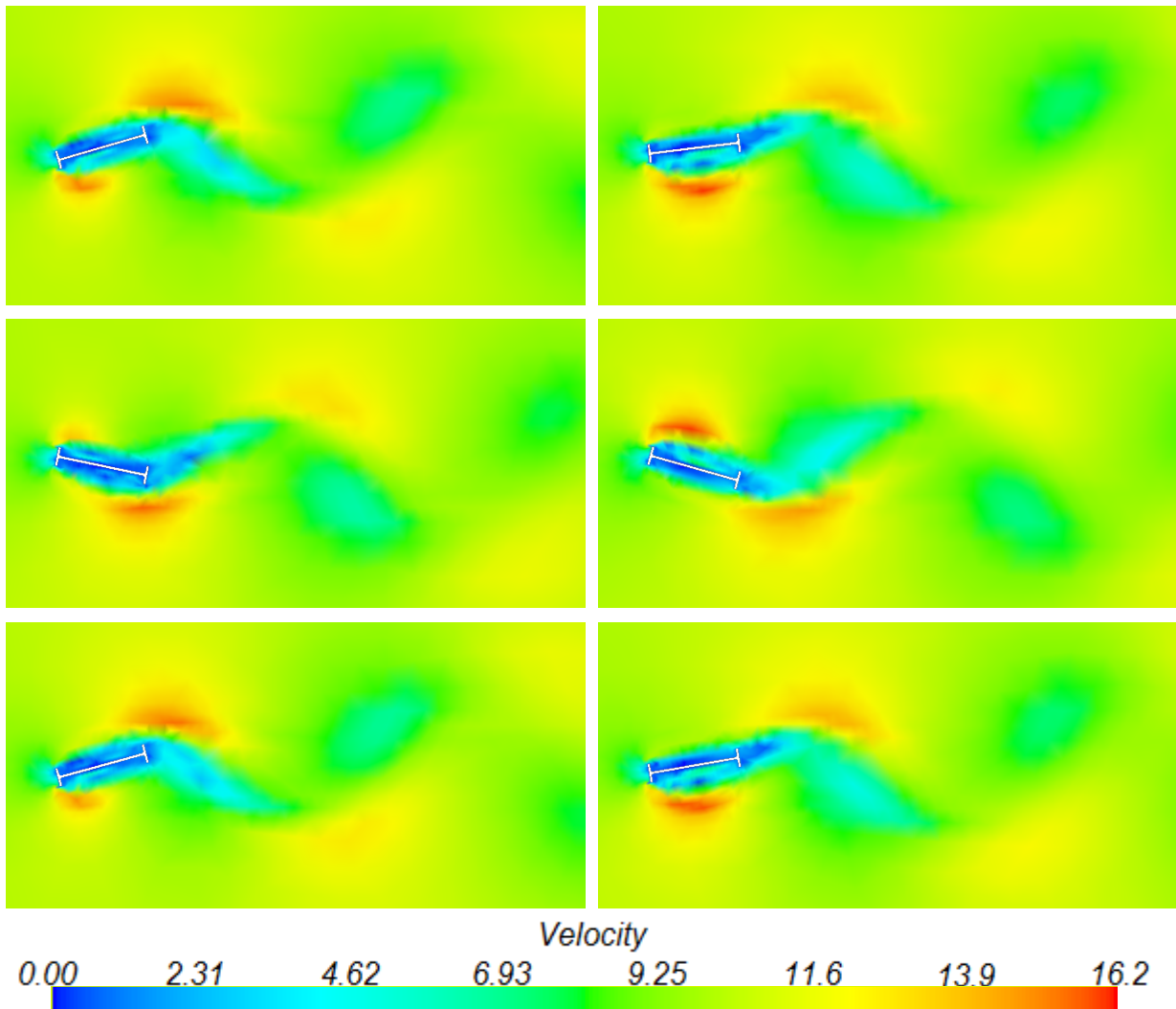


Figure 28: Magnitude of Velocity

6. CONCLUSIONS

This work explore the interconnection of BGs models with CFD codes with the goal of resolving problems of interaction between fluid and dynamic systems. A high-level, interactive and productive Python interface have been used. Strongly coupled partitioned staged algorithm was implemented in this interface. Some examples, with complex phenomena as *lock-in*, *galloping* and *flutter* have been presented. Future work will be directed towards to problems of vehicle aerodynamic attached to vehicle dynamics models.

7. REFERENCES

- R. Blevins, Flow Induced Vibration, Van Nostrand Reinhold Company, New York, 1977.
- W. Dettmer and D. Peric. A computational framework for fluid-rigid body interaction: Finite element formulation and applications. *Comput Methods Appl Mech Engrg*, 195:1633–1666, 2006.
- G. Filippini, N. Nigro, M. Storti, R. Paz. Vortex-Induced Vibration Around a Cylinder at Low Reynolds Numbers. *Mecánica Computacional - Vol. XXV*. AMCA, 2006. ISSN 1666-6070.
- G. Filippini, D. Delarmelina, J. Pagano, J. Alianak, S. Junco and N. Nigro. Dynamics of Multibody Systems with Bond Graphs. *Mecánica Computacional - Vol. XXVI*. AMCA, 2007b.
- D. Karnopp, D. Margolis, R. Rosenberg. Modeling and Simulation of Mechatronic Systems, A Wiley-Interscience Publication, New York, 2000. ISBN 0-471-33301-8
- E. Lopez, N. Nigro, M. Storti, and J. Toth. A minimal element distortion strategy for computational mesh dynamics. *Int J Num Meth Engng*, 2006.
- R. Piperno and C. Farhat. Partitioned procedures for the transient solution of coupled aeroelastic problems. Part II: Energy transfer analysis and three-dimensional applications. *Comput Methods Appl Mech Engrg*, 190:3147-3170,2001
- M. Storti, N. Nigro, and R. Paz. Stability and time integration of partitioned fluid-structure interaction problems at supersonic mach numbers. *Journal of Sound and Vibration*, 0:1–1, 2006.